GEOMETRY EFFECT ON GRAPHENE NANORIBBON BASED TRANSISTOR

SAYED NOROLLAH HEDAYAT, MOHAMMAD TAGHI AHMADI,

HASSAN SEDGHI & HADI GODARZI

Department of physics, Faculty of science, Urmia University, Urmia, Iran

ABSTRACT

Graphene has incredible carrier transport property with high application opportunity at single molecule level, which composes it as promising materials on Nano electronic application. In order to develop the new device such as graphene nanoribbon transistor, Carbon Nanotube Field Effect Transistor (CNTFET) and Nanowire based devices, it is essential to investigate the quantum limit in low dimensional systems. In this paper transmission coefficient of the schottcky structure in the graphene based transistor based on the width of semiconducting channel is modeled additionally its quantum properties due to the structural parameters are analyzed. Also one dimensional quantum current in the presence of the wave vector approximation for monolayer graphene nanoribbon (MGNR) is presented.

KEYWORDS: Quantum Current, Degenerate and Nondegenerate Approximation, Graphene Nanoribbons, Transmission Coefficient

INTRODUCTION

Recently graphite based materials such as grapheme nanoribbon has been studied extensively [1, 2]. Graphene nanoribbon (GNR) as a monolayer graphite with nanometer width indicates excellent electrical [3] and optical [4, 5] properties. Thus in all related fields including transistor fabrication [6] interconnecting circuitry [7], electromechanical switches [8] infrared emitters and bio- sensors have been employed widely [8]. Furthermore, the electronic structure of graphene and its low scattering rate lead in desirable electronic transmission, compatibility of doping and utilization on electrostatic area. Particular nature of graphene's charge carriers made it important component [11, 12]. Even long mean free path and also electron–electron interactions with high level of electron scattering exist in graphene [18, 19]. By considering all these unique properties of carbon nanostructures specially GNRs with distinguished properties it is completely accepted as a promising component in future electronic technology [20, 21].

As shown in figure 1 the schematic of GNR transistor with two schottcky is considered this structure can be made by top-down fabrication method.
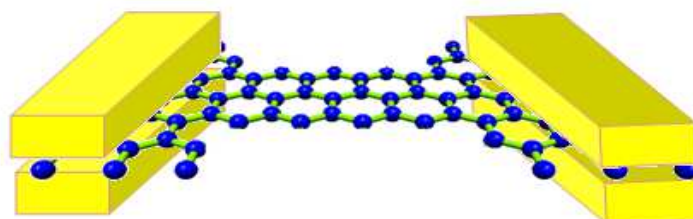

**Figure 1: Schematic of Two Schottcky Contacts of Metallic
Graphene with Semiconducting in the Channel Region**

In an atomic level the approach of top-down is so efficient to particular control over the width and edge termination of the nanoribbon. And the fabrication of mentioned structure can be achieved by oxygen plasma etching [28, 29, 30] the proposed structure is employed as a transistor platform in the analytical modeling.

MODEL

By using Tight-binding method GNRs in ab-initio the non-zero direct band gap of hydrogen termination of either armchair or zigzag shaped edges have been estimated. The proportionality of two parameters in GNRs width and E_g (band gap energy) has been reported. Numerous computation for various structures by moving one layer over the other in which the atoms are locating at the center of hexagons in the upper layer and in the direction of the infinite edge has been done [25,26, 27]. The engineered graphene with armchair structure with 0.22 eV has been reported. By increasing the thickness of the sample E_g starts to decrease and finally become zero. This observation provides a promising proportionality of graphene band gap engineering. Band energy calculation as a key fundamental parameter based on the tight- binding method has been reported as:

$$E(\vec{k}) = \pm t\sqrt{1 + 4\cos\left(\frac{k_x 3a_{c-c}}{2}\right)\cos\left(\frac{k_y \sqrt{3}a_{c-c}}{2}\right) + 4\cos^2\left(\frac{k_y \sqrt{3}a_{c-c}}{2}\right)}$$

(1)

Where k_x, k_y are the wave vector next to the extent of the nanoribbon and ac-c is the carbon-carbon band length, on the other hand the presented model can be modified as [19]:

$$E(\vec{k}) = \pm\frac{3a_{c-c}t}{2}\sqrt{k_{x^2} + \beta^2}$$

(2)

Where $\beta = \frac{2\pi}{a_{c-c}\sqrt{3}}\left(\frac{p_i}{N+1} - \frac{2}{3}\right)$ the quantized wave vector and N is the number of dimmer appearance which, determine the thickness of the ribbon and p_i is the sub band directory. The modified one dimensional dispersion relation for the further development is considered and the transmission amplitudes for a single square barrier centered at the origin with height V_0 and width bas shown in the figure 2 is analytically modeled.
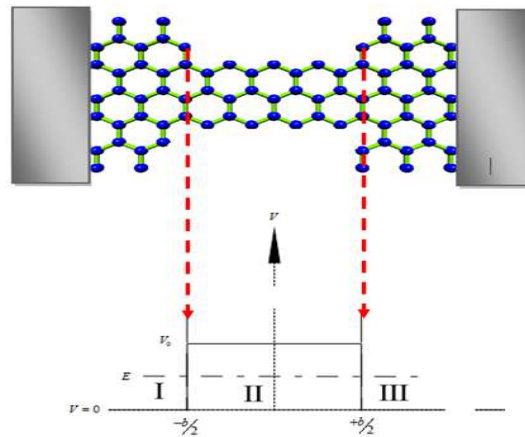

Figure 2: Channel Region Barrier in GNR based Contact

The transistor operation can be modeled in the form of three different regions as shown in figure 4 which leads to the Schrödinger equation result for potential of each region as:

$$V(x) = \begin{cases} 0 & , \quad x \langle \dfrac{-b}{2} \\ V_0 & , \quad \dfrac{-b}{2} \langle x \langle \dfrac{b}{2} \\ 0 & , \quad x \rangle \dfrac{b}{2} \end{cases} \Rightarrow \psi(x) = \begin{cases} A_n e^{ikx} + B_n e^{-ikx} & , \quad x \langle \dfrac{-b}{2} \\ C e^{-Kx} + D e^{Kx} & , \quad \dfrac{-b}{2} \langle x \langle \dfrac{b}{2} \\ A_{n+1} e^{ikx} + B_{n+1} e^{-ikx} & , \quad x \rangle \dfrac{b}{2} \end{cases} \tag{3}$$

Where wave number in first and third regions are $k = \sqrt{\dfrac{2mE}{\hbar^2}}$, and the wave number in channel region is

$K = \sqrt{\dfrac{2m(V_0 - E)}{\hbar^2}}$, therefore the boundary condition implies that the constant parameters can be modeled as:

$$\begin{pmatrix} A_{n+1} \\ B_{n+1} \end{pmatrix} = \begin{pmatrix} e^{-K\left(\frac{b}{2}\right)} & e^{K\left(\frac{b}{2}\right)} \\ -Ke^{-K\left(\frac{b}{2}\right)} & Ke^{K\left(\frac{b}{2}\right)} \end{pmatrix} \begin{pmatrix} e^{ik\left(\frac{b}{2}\right)} & e^{-ik\left(\frac{b}{2}\right)} \\ ike^{ik\left(\frac{b}{2}\right)} & -ike^{-ik\left(\frac{b}{2}\right)} \end{pmatrix}^{-1} \begin{pmatrix} e^{ik\left(\frac{-b}{2}\right)} & e^{-ik\left(\frac{-b}{2}\right)} \\ ike^{ik\left(\frac{-b}{2}\right)} & -ike^{-ik\left(\frac{-b}{2}\right)} \end{pmatrix} \begin{pmatrix} e^{-K\left(\frac{b}{2}\right)} & e^{K\left(\frac{b}{2}\right)} \\ -Ke^{-K\left(\frac{b}{2}\right)} & Ke^{K\left(\frac{b}{2}\right)} \end{pmatrix}^{-1} \begin{pmatrix} A_n \\ B_n \end{pmatrix} \tag{4}$$

The transmission coefficient as a main transport indicator in electrical need to be investigated while wave propagation in an intermediate part as a transistor channel is interrupted by junction barrier. The transmission coefficient has been explained by transmission amplitude, concentration and total power of a transmitted wave as:

$$t = \frac{-4kKe^{-ikb}}{4kK\cosh(bK) + 2i(k^2 - K^2)\sinh(bK)} \tag{5}$$

The transmission coefficient is a scale of how an electromagnetic wave (light) propagates throughout a material [30] which is the transmission amplitude to power of two therefore the transmission coefficient T can be calculated as:

$$T = |t|^2 = \frac{4\dfrac{K^2}{k^2}}{-1 + 2\dfrac{K^2}{k^2} - \dfrac{K^4}{k^4} + \left(1 + 2\dfrac{K^2}{k^2} + \dfrac{K^4}{k^4}\right)\cosh^2(bK)} \tag{6}$$

Where b is the length of the barrier, the wave vector k outside the barrier is a real quantity for all positive energies E of the electron. The conduction band minimum in the region outside the barrier is taken as the zero of energy. Since the conduction band minimum of the barrier is above that of the region outside hence for certain energies of the electron ($E \langle V_0$) the wave vector K will be imaginary and for energies above V_0 ($E \rangle V_0$) it will be real. Thus the energy is divided into two regions, ($E \langle V_0$) for non-classical transition by tunneling and ($E \rangle V_0$) where transition can take place even under classical conditions. Since k and K are both dependent on effective mass and energy, hence for different material pairs the variation of the transmission coefficient for energy values with respect to the barrier height will be

different [33, 34,35]. For energies with transmission value equal to 1 the barrier becomes transparent which is called Ramseur Towns effect. When the electron energy E is less than the barrier height Vo the situation is somewhat different [36].

The transmission coefficient of electrons through a potential barrier is important for studying the leakage current in MOSFETs with dimensions in the nanometer range. It is also a crucial parameter for studying the behavior of multiple quantum well structures where the barrier is sandwiched between two coupled quantum wells. When both the well and barrier regions are in the nanometer range we expect further quantization of the energy levels. As the barrier width decreases the tunneling increases and transmission coefficient value rises with electron energy. For $\left(E_n = \dfrac{E}{V_0} \langle 1 \right)$, the transmission coefficient increases from 0 to 1 in a non-linear fashion by increasing the wave number as shown in figure 3,4 for different regions.
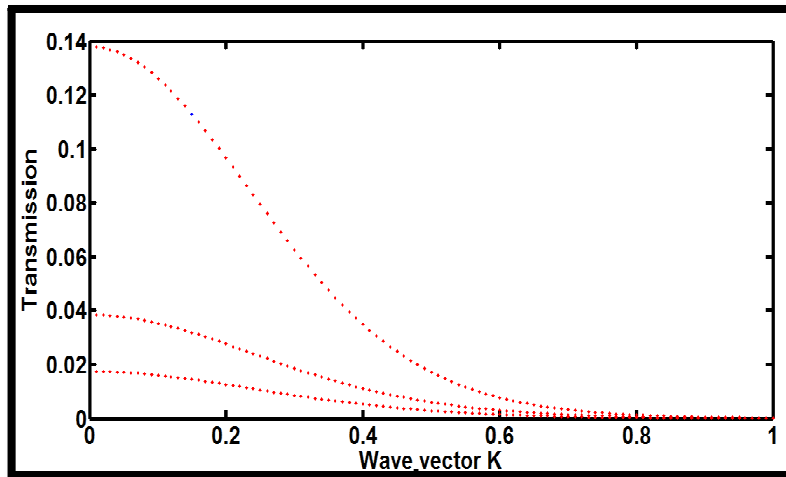

Figure 3: Transmission for Different K Values in the GNR at Channel Region
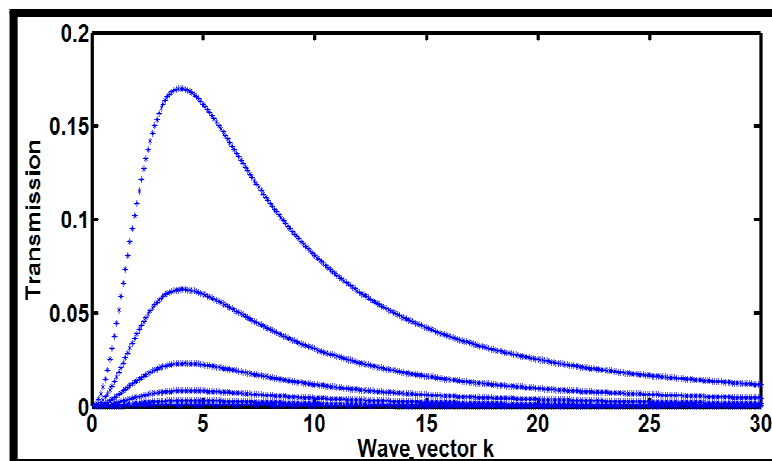

Figure 4: Transmission for different k Values in the GNR at First and Third Regions

As shown in figure 3 and figure 4 if the energy of electron in each region is changed within allowed values the transmission coefficient is varied accordingly. Additionally beyond the normalized energy $\left(E_n = \dfrac{E}{V_0} \right) \rangle 1$, the resonance in

the transmission coefficient is observed as shown in figure 8.

On the other hand, as show in figure 5 and figure 6 the manipulation of channel region will affect the transmission property sharply consequently for each pair, the transmission coefficient is lower for wider wells as expected.
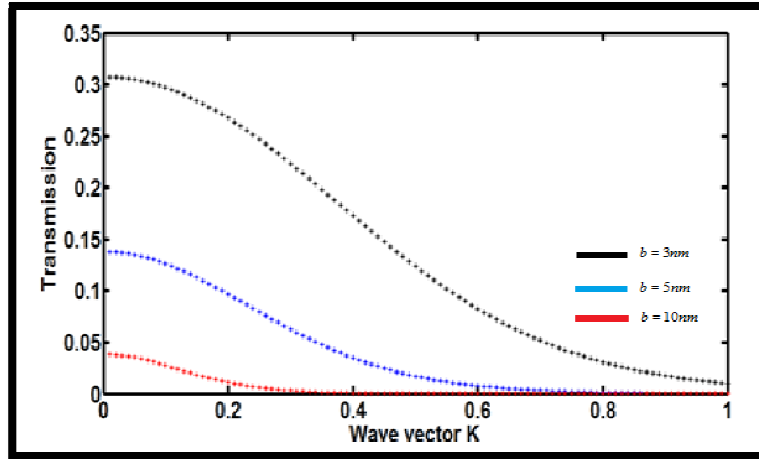

Figure 5: The Transmission Variation Based on the Channel Region Length (Black Line Indicates Channel Length 3, Blue Line for Channel Length 5nm and Red Line Shows Channel Length Equal to 10 nm)
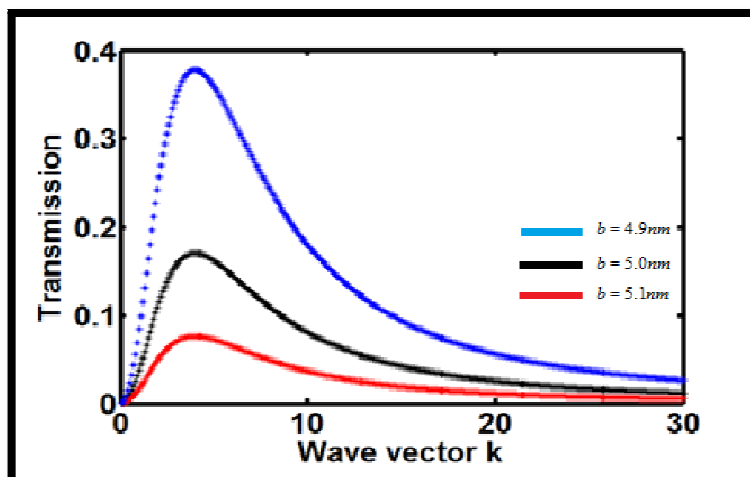

Figure 6: The Transmission Variation based on the Channel Region Length (Black Line Indicates Channel Length 5nm, blue Line for Channel Length 4.9nm and Red Line Shows Channel Length Equal to 5.1 nm)

It is discovered that the performance of the transmission $T(E)$ is increased rapidly while the energy of the electron is less than the barrier height energy (E<V0) on the other hand for the energies more than the potential barrier the transmission is saturated at 1 as expected. But the presented model needs to be modified for this region to get the accurate results. In the presence of k^2 and K^2 the transmission can be modified as:

$$T(E) = \frac{4\dfrac{V_0 - E}{E}}{-1 + 2\dfrac{V_0 - E}{E} - \left(\dfrac{V_0 - E}{E}\right)^2 + \left(1 + 2\dfrac{V_0 - E}{E} + \left(\dfrac{V_0 - E}{E}\right)^2\right)\cosh^2\left(\alpha b \sqrt{V_0 - E}\right)}$$

(7)

Based on the presented model the transmission is analyzed and the numerical result indicates that channel length affects transmission characteristics very fast. As shown in figure (7) the transmission coefficient for a barrier of height V0=-1ev and width 1nm up to 5 nm varies by channel length. It is notable that for each channel region the optimum electron energy is different and the maximum transmission occurs at 0.45 eV, 06eV, 0.75 eV and 0.9eV for channel lengths 1nm, 2nm, 3nm and 5 nm respectively. The analyze of the numerical plot indicates that by increasing the channel region optimum energy is closer to the barrier height.
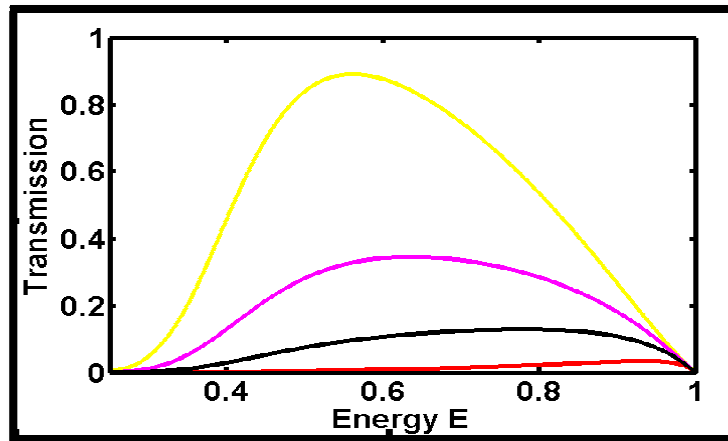

Figure 7: The Transmission Variation for Energies Less Than Barrier High

It is observed that for all cases the saturation part occurs at E>V0 as shown in figure (8) therefore for energies more than this value the transmission need to be considered as one.
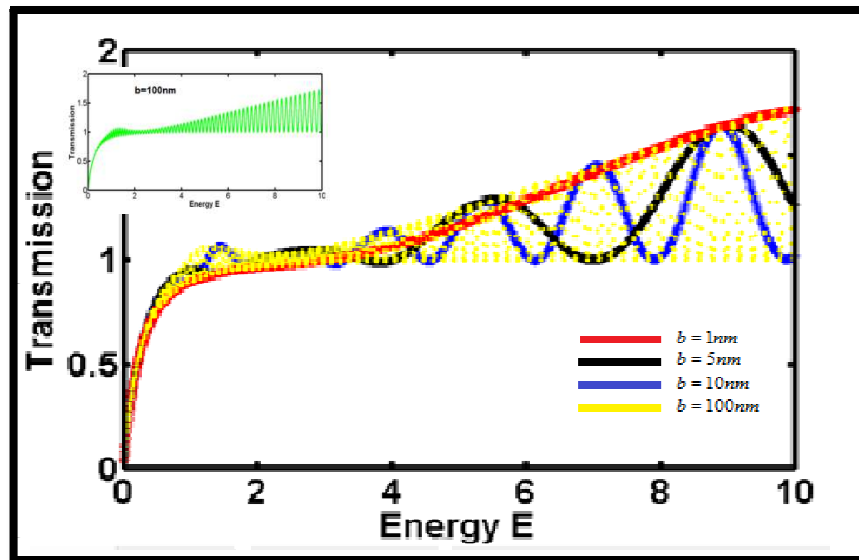

Figure 8: The T-E Characteristic with Channel Length Variation for Energies More than Barrier Height
As a Result, the Quantum Current Based on the Landauer Formalism is developed as:

$$I_q = \int_0^\eta T(E)F(E)dE$$

(8)

Where F (E) is Fermi Dirac distribution functions which demonstrate the probability of occupied levels at energy E and leads the current calculation in the form of:

$$I_q = \int_0^\eta \frac{4\left(\frac{\beta}{T}-1\right)}{-1+2\left(\frac{\beta}{T}-1\right)-\left(\frac{\beta}{T}-1\right)^2+\left(1+2\left(\frac{\beta}{T}-1\right)+\left(\frac{\beta}{T}-1\right)^2\right)\cosh^2\left(\alpha b\sqrt{\frac{V_0}{\beta}}(\beta-T)\right)}\frac{1}{1+e^{x-\eta}}dx$$

(9)

We define $\frac{E-E_g}{k_B T}=x$, $\frac{E_g-E_f}{k_B T}=-\eta$, $\alpha=\sqrt{\frac{2m}{\hbar^2}}$, $\beta=\frac{2V_0}{3K_B}$, K_B is Boltzmann's constant and T is

temperature. The temperature dependency on the quantum current is shown in Figure (9), where the degenerate regime is being highlighted because the Nano scale transistors are operating in this regime.
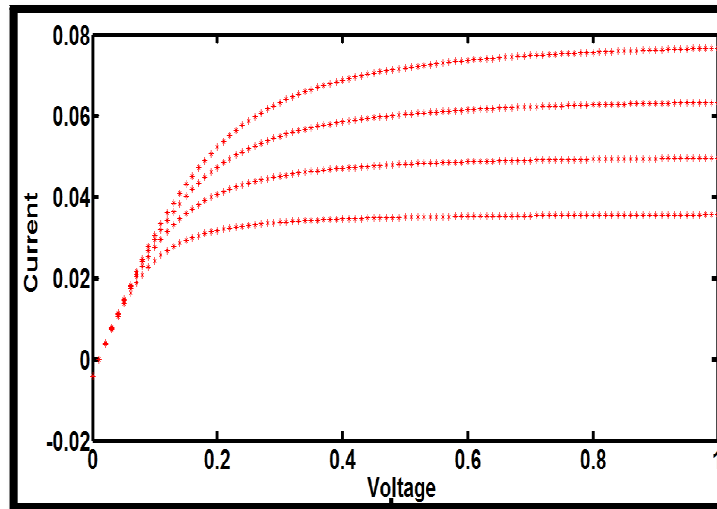

Figure 9: Current –Voltage Characteristic of GNR Transistor Based on the Presented Model

As shown in figure 9 the Ohmic response on Current –Voltage (I-V) characteristic for small value of applied bias is observed and the saturation current for the higher voltages are reported.

CONCLUSIONS

Graphene nanoribbon derived from the two-dimensional Graphene has a great impact on the nanoscale transistor performance. Its application on nanoscale device fabrication is expected to run the nanotechnology engine. Among the issues highlighted for GNR is the GNR based device quantum current which contributes to the faster transistor operation and thus expected to alter the carrier mobility. The main parameter that plays important role on device characteristic is transmission coefficient. In this paper quantum current of Monolayer Graphene Nanoribbon (MGNR) based on transmission calculation is modeled and the electronic property due to the dependence on structural parameter such as channel length is analyzed.

ACKNOWLEDGMENT

REFERENCES

1. Y. G. Gogotsi, et al., "Materials: Transformation of diamond to graphite," Nature vol. 401, pp. 663-664, 1999.

2. T. Irifune, et al., "Materials: Ultrahard polycrystalline diamond from graphite," Nature, vol. 421, pp. 599-600, 2003.

3. P. L. McEuen, et al., "Single-walled carbon nanotube electronics," Nanotechnology, IEEE Transactions on vol. 1, pp. 78-85, 2002.

4. J. A. Misewich, et al., "Electrically induced optical emission from a carbon nanotube FET," Science, vol. 300, pp. 783–786, 2003.

5. J. Chen, et al., "Bright infrared emission from electrically induced excitons in carbon nanotubes," Science, vol. 310, pp. 1171–1174, 2005.

6. A. Javey, et al., "Ballistic carbon nanotube field-effect transistors," Nature vol. 424, pp. 654-657, 2003.

7. J. Li, et al., "Bottom-up approach for carbon nanotube interconnects," Appl. Phys. Lett., vol. 82, pp. 2491–2493, 2003.

8. J. E. Jang, et al., "Nanoelectromechanical switches with vertically aligned carbon nanotubes," Applied Physics Letters,,vol. 87, pp. 163114 -163116, 2005.

9. J. Kong, et al., "Nanotube molecular wires as chemical sensors," Science, vol. 287, pp. 622–625, 2000.

10. A. K. Geim and K. S. Novoselov, "The rise of graphene," Nature Materials, vol. 6, pp. 183 - 191, 2007.

11. T. O. Wehling, et al.,Molecular Doping of Graphene," Science Nano Lett., vol. 8, pp. 173–177, 2004.

12. D. J. K. S. Novoselov, F. Schedin, T. J. Booth, V. V. Khotkevich, S. V. Morozov and A. K. Geim, "Two-dimensional atomic crystals," Proc. Natl Acad. Sci, vol. 102, pp. 10451–10453, 2005.

13. F. schwierz, "graphene transistors," Nature Nanotechnology, vol. 5, pp. 487-496, 2010.

14. S. Entani, et al., "Interface Properties of Metal/GrapheneHeterostructures Studied by Micro-Raman Spectroscopy," Journal of Physical Chemistry C, vol. 114, pp. 20042-20048, 2010.

15. A. H. Castro Neto, et al., "The electronic properties of graphene," Rev. Mod. Phys, vol. 81, pp. 109–162, 2009.

16. A. V. Rozhkova, et al., "Electronic properties of mesoscopicgraphene structures: Charge confinement and control of spin and charge transport " Physics Reports, vol. 503, pp. 77-114 2011.

17. Y. H. Hu, et al., "Thinnest Two-Dimensional Nanomaterial—Graphene for Solar Energy," ChemSusChem, vol. 3, pp. 782 – 796, 2010.

18. F. Guineaa, et al., "Electronic properties of stacks of graphene layers," Solid State Communications, vol. 143, pp. 116-122, 2007.

19. H. Li, et al., "Carbon Nanomaterials for Next-Generation Interconnects and Passives: Physics, Status, and Prospects," IEEE Transactions on Electron Devices, vol. 56, pp. 1799-1821, 2009.

20. M. Lundstrom and J. Guo, "Nanoscale transistors: device physics, modeling and simulation," Springer, Birkhäuser- Technology & Engineering - 217 pages, 2006.

21. K. Nakada, et al., "Edge state in graphene ribbons: Nanometer size effect and edge shape dependence," Phys. Rev. B, vol. 54, pp. 17954-17961, 1996.

22. Y. Takane, "Anomalous Enhancement of the Boltzmann Conductivity in Disordered Zigzag GrapheneNanoribbons," Journal of the Physical Society of Japan, vol. 79, 2010.

23. H. Kumazaki and D. S. Hirashima, "Spin-Polarized Transport on Zigzag GrapheneNanoribbon with a Single Defect," Journal of the Physical Society of Japan, vol. 78, 2009.

24. E. Watanabe, et al., "Ballistic thermal conductance of electrons in graphene ribbons," Phys. Rev. B vol. 80, 2009.

25. H. Cheraghchi and H. Esmailzade, "A gate-induced switch in zigzag graphenenanoribbons and charging effects," Nanotechnology vol. 21, 2010.

26. S. S. Yu, et al., "Electronic Properties of Nitrogen-/Boron-Doped GrapheneNanoribbons With Armchair Edges "Nanotechnology, IEEE Transactions on, vol. 9, pp. 78 - 81 2010.

27. A. K. G. K.S. Novoselov, S.V. Morozov, D. Jiang, M.I. Katsnelson, I.V. Grigorieva, S.V. Dubonos, A.A. Firsov, "Two-Dimensional Gas of Massless Dirac Fermions in Graphene," Nature 438:197, 2005.

28. Zydziak, N., et al., Modular ambient temperature functionalization of carbon nanotubes with stimuli-responsive polymer strands. Polymer Chemistry, 2013. 4(5): p. 1525-1537.

29. Zhang, Y.-Y., et al., Impurities in graphene.Physica Status Solidi a-Applications and Materials Science, 2010. 207(12): p. 2726-2738.

30. S.N.hedayat and M.T.ahmadi, et al., Quantum Current Modelling on GrapheneNanoscrolls. University of Diyala Dec 2015, pp-599-605.

31. Nakada, K., M. Fujita, et al., "Edge state in graphene ribbons: Nanometer size effect and edge shape dependence," Physical Review B 54(24): 17954 (1996).

32. Areshkin, D. A., D. Gunlycke, et al., "Ballistic Transport in GrapheneNanostrips in the Presence of Disorder: Importance of Edge Effects," Nano Letters 7(1): 204-210 (2006).

33. Physics of Quantum Well Devices, B.R.Nag, Klewer Academic Publishers.

34. T.Kuhn and G.Mahler, PhysicaScripta, 38, 216 (1988).

35. Martin David Treharne Evans, Quantum Mechanical Tunnelling, July (2012)

36. Xi.Chen and Chun-Fang Li, Eur. Phys. J. B. 46, 433 (2005).

37. J. Gain, M. Das Sarkar and S. Kundu, Energy and Effective Mass Dependence of Electron Tunnelling Through Multiple Quantum barriers in Different Heterostructures. West Bengal University of Technology, BF-142 Salt Lake Sector-I, Calcutta – 700064, (2003).